THE JOURNAL OF PHYSICAL CHEMISTRY B

Article

Cite This: J. Phys. Chem. B 2019, 123, 5536−5544

pubs.acs.org/JPCB

Analysis of Correlated Dynamics in the Grotthuss Mechanism of Proton Diffusion

Sean A. Fischer* and Daniel Gunlycke

Chemistry Division, U.S. Naval Research Laboratory, Washington, D.C. 20375, United States

Supporting Information

ABSTRACT: Using a large set of ab initio molecular dynamics trajectories we demonstrate that the mechanistic details of aqueous proton diffusion are insensitive to finite size effects. Furthermore, we show how correlation in the proton hopping direction is related to the presolvation of the hydronium ion. Specifically, we observe a dependence of the probability for the excess proton to return to its previous hydronium ion on whether that hydronium ion was accepting a hydrogen bond from a fourth water molecule at the time the excess proton left. The dynamics of this fourth water molecule was previously linked to the net displacement of the proton, and our analysis shows that this connection is due to the changes in the hopping probability that we calculate. Additionally, we show how our simulated dynamics with correlations that imply a faster time scale are compatible with recent spectroscopy results that point to a slower hopping time scale by looking closely at which proton transitions are being taken into consideration. Finally, we show that the correlation in proton hopping directions is not strongly influenced by interactions among hydronium ions.

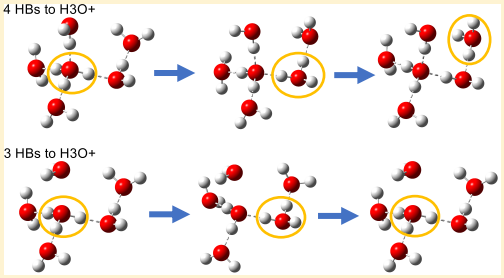

INTRODUCTION

The Grotthuss mechanism refers to the shuttling of protons through the hydrogen bond network of water. This proton hopping process is what gives rise to the anomalously large diffusion coefficients of the hydronium and hydroxide ions.[1] Due to the ubiquity of aqueous proton dynamics in chemistry and biology, a prodigious amount of work has gone into understanding the details of the Grotthuss mechanism.[1−40]

One key insight has been the role of hydrogen bond dynamics, particularly between the first and second solvation shell water molecules, in facilitating proton hopping.[7−10,12,13,20,22,24] A plethora of computational studies have coalesced around the picture that a hydrogen bond to one of the water molecules involved in the primary solvation of a hydronium ion (H_3O^+) needs to break in order to enable proton transfer from the hydronium ion to this water molecule.[7−9,13,20,22,24] Recent computational studies have expanded this view, suggesting that the presence of a weak hydrogen bond being donated to the hydronium ion leads to periods of greater net displacement of the excess proton as compared to when there is no hydrogen bond being donated.[29,30] This could be indicative of correlations in the underlying proton hopping dynamics.

In our own previous work, we used a large set of ab initio molecular dynamics simulations to show that there is correlation in the proton hopping directions.[40] While not the first time that this correlation was suggested,[4] our work provided direct evidence of its existence. This correlation is important as the benchmark experimental results used to establish a time scale for the Grotthuss mechanism have been interpreted in terms of a simple random walk model,[2−4,7] which is invalid in the presence of correlations. We showed that using a correlated random walk model instead of the simple model gives a time scale ∼3 times faster than previously reported.[40]

At the same time, a series of recent vibrational spectroscopy experiments have asserted a time scale of 1−2 ps for the Grotthuss mechanism.[35,37,38] Since the analysis of the spectroscopy experiments did not rely on a random walk model to obtain the quoted time scale, an apparent conflict exists between the ultrafast spectroscopy and the NMR/conductivity measurements interpreted with the aid of ab initio molecular dynamics.

In the present work, we have expanded upon our previous simulations in order to first establish that the observed correlation in the proton hopping directions was not an artifact of the size of the simulations. Second, we demonstrate how the correlation in proton hopping directions provides a natural explanation of the previously observed correlation between net displacement of the proton and the hydronium ion accepting a hydrogen bond. Digging deeper, we use a regression analysis to disentangle the influences of the hopping probability and the dynamics of this fourth water molecule on proton displacement. We then show that the apparent conflict between our previous result and the vibration spectroscopy can be resolved by a careful consideration of which protons hops are considered in the analysis. Finally, we present evidence that shows the correlation in the proton hopping directions is not

Received: March 19, 2019
Revised: June 7, 2019
Published: June 10, 2019

DOI: 10.1021/acs.jpcb.9b02610
J. Phys. Chem. B 2019, 123, 5536−5544

sensitive to hydronium−hydronium interactions, which may have implications for its dependence on concentration.

METHODS

For our molecular dynamics simulations we considered three systems consisting of 31 water molecules and 1 hydrochloric acid (HCl) molecule in a cubic box with an edge length of 9.87 Å, 62 water molecules and 2 HCl molecules in a cubic box with an edge length of 12.45 Å, and 93 water molecules and 3 HCl molecules in a cubic box with an edge length of 14.24 Å. These sets of simulations are referred to as W32, W64, and W96 in the rest of the Article. Increasing the number of HCl molecules as the simulation size increased ensured that any finite size effects would not be confounded with concentration dependent properties. All calculations were performed with Quantum Espresso v5.4 using the CP module.[41] The electronic structure was described by the PBE exchange-correlation functional in conjunction with ultrasoft pseudopotentials with 25 and 200 Ry cutoffs for the wave functions and charge density, respectively.[42−45] We note that while there are well-known deficiencies in the ability of the PBE functional to describe liquid water,[46,47] our previous study showed that the correlation in the proton hopping directions was insensitive to the choice of functional, a result that is in line with the insensitivity of the details of proton diffusion to the level of theory observed by others.[20,21,28,39]

A Nose−Hoover chain with 4 thermostats and a characteristic frequency 140 THz was used to simulate a canonical ensemble with a target temperature of 300 K. For our Car−Parrinello molecular dynamics,[48] we used a time step of 4 atomic units (~0.097 fs) and a fictitious electron mass of 300 m_e. Data were sampled every 10 time steps, and the first picosecond of each 8 ps trajectory was discarded for equilibration. The W32 system (31 H_2O/1 HCl) is the same from our previous study[40] and includes 500 independent trajectories. For the W64 system (62 H_2O/2 HCl), we ran 250 independent trajectories. Finally for the W96 system (93 H_2O/3 HCl), we ran 167 independent trajectories.

The initial coordinates for each trajectory were sampled from separate 5 ps trajectories that used the same computational parameters. The starting configurations for these initial trajectories were constructed by first randomly placing molecules in the simulation cell (taking care not to overlap the molecules). The random configurations then had their geometries optimized, and the relaxed configurations served as the starting point for the initial trajectories. Using initial configurations generated from trajectories run with the same level of theory and starting from geometrically relaxed structures ensured that our production trajectories did not have a long equilibration time, which is verified later in the Article.

To assess the dependence of the results on the level of theory, we also performed analyses on the smaller sets of trajectories from our previous work[40] for the PBE,[42] PBE-D2,[49,50] revPBE,[42,51] BLYP,[52,53] BLYP-D2,[49,50,52,53] and optB88 exchange-correlation functionals at cutoffs of 50 and 400 Ry. The optB88 results are new to this work. These were done with 32 molecules and 10 trajectories each. The remaining computational parameters were the same as the other simulations. To assess convergence with respect to trajectory length, we ran 10 additional trajectories with the W32 system, each 100 ps in length (all of the parameters were the same as the original 500 W32 simulations). In total, we had almost 9 ns of simulation time and over 1500 individual proton trajectories when the multiple proton trajectories per simulation for the W64 and W96 systems are considered.

In order to analyze the dynamics of the aqueous proton, we need a method for defining where the positive charge is located during the trajectory. The simplest approach is to first assign two hydrogen atoms to every oxygen atom based on distance. The remaining unassigned hydrogen atom can then be assigned to its nearest oxygen atom. This creates a hydronium ion, which can be used as the cation. However, this simple approach is flawed and will result in an overabundance of proton hopping events due to the very low barrier for an excess proton to move between neighboring oxygen atoms. This "proton rattling" has been recognized as a problem for the analysis of proton dynamics before, and the most common method for dealing with it has been to not count any proton hops that are undone by the next hop.[20,21,24,31,54] For example, if the proton hopped from oxygen atom A to oxygen atom B, and then subsequently hopped back to oxygen atom A, the hops from A to B and then B back to A would be discarded and oxygen atom A would be considered the host for the excess proton over that entire time.

This approach is problematic for an unbiased analysis. Though the intention of disregarding hops that are undone by a subsequent hop is to reduce proton rattling, a backward hop is a perfectly legitimate move in terms of a random walk. Therefore, this approach does not guarantee that the neglected hops correspond to rattling events. This means that the a priori disregard of certain hops could bias the ensuing analysis. In our own testing we have observed this with situations where the above procedure leads to an oxygen atom being designated as the hydronium ion when one of its neighbors is clearly hosting the excess proton.

Another approach that has been used in the literature for analyzing hopping is varying the sampling rate from the trajectory.[29] The idea behind changing the amount of time between when frames of the trajectory are analyzed is that if the time between samples is too small, too much weight will be given to rattling events. However, windowing the trajectory will only be effective for eliminating rattling events if both the proton rattling and the "real" hops occur in a periodic fashion with a well-defined interval. Otherwise, the windowing can still eliminate "real" hops while keeping rattling events. This is illustrated in Figure 1 where we show the average hopping distance as a function of the time between samples. As the time between samples increases, so does the average hopping distance. So while we would certainly end up with fewer hops

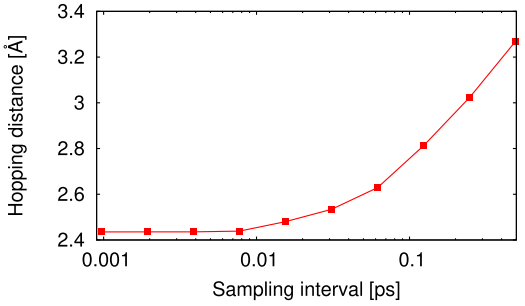

Figure 1. Change in the average proton hopping distance as the trajectory sampling rate is lowered. This was calculated with data from the W32 simulation set.

DOI: 10.1021/acs.jpcb.9b02610
J. Phys. Chem. B 2019, 123, 5536−5544

in a given trajectory by lowering the sampling rate, we would also miss a large portion of the fundamental dynamics of the proton.

In our previous work,[40] we introduced a new method to define the protonic cation at every step, which served to eliminate most if not all of the proton rattling without rejecting certain types of hops from the beginning. Our approach follows that laid out above for the first frame in a trajectory; however, in subsequent frames, a hop is only counted if the excess proton, identified as the unassigned hydrogen atom after all oxygen atoms have been assigned two hydrogen atoms, is not one of the three hydrogen atoms that constituted the hydronium ion from the previous step. This allows the excess proton to vibrate freely between two oxygen atoms without changing the identity of the hydronium ion every time the proton crosses the midpoint. Doing so allows our method to accommodate the special-pair dance of the excess proton.[22]

The special-pair dance refers to changes in which the solvating water molecule is closest to the hydronium ion and thereby is involved in the relatively free motion of the excess proton between oxygen atoms. The identity of the special partner for a hydronium ion changes on average several times before a new oxygen atom becomes identified as the center of the hydronium ion. Our method was specifically designed to account for the dynamics of the special-pair dance. In fact, another way to view our algorithm is to say that we identify the partners of the special-pair dance in every frame and then choose which of those two will be designated the hydronium ion in such a way that the number of proton hops over the trajectory is minimized. The hydronium ion oxygen atom was used as the location of the positive charge in the analysis.

RESULTS AND DISCUSSION

Before discussing correlations in the proton dynamics, we begin with a general characterization of our simulations. As mentioned previously, the PBE exchange-correlation functional is known to have deficiencies when it comes to the description of water. Perhaps the most well-known is its overstructuring as exemplified in the oxygen−oxygen radial distribution function shown in Figure 2 (we have collected several other radial distribution functions for the studied systems in the Supporting Information). As was observed in past simulations,[55] increasing the size of the simulation cell serves to soften the water structure somewhat, but the simulated water still displays characteristics of being in a supercooled state.

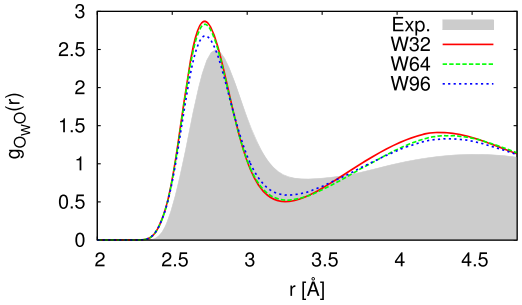

Figure 2. Water oxygen−oxygen radial distribution functions. The radial distribution function is calculated between the oxygen atoms of those molecules identified as water molecules and every other oxygen atom. The experimental results for bulk water are from Soper.[56]

Going along with the tighter structure of the simulated water, the calculated diffusion coefficients for water appear to be underestimated as compared to the experimentally determined self-diffusion coefficient of water, although the calculated proton diffusion coefficient appears to be overestimated at the same time. In Figure 3 we show the calculated diffusion coefficients of water (taken as the diffusion coefficient of the oxygen atom) and the excess proton as functions of the inverse box length. Additional data related to the calculated diffusion coefficients can be found in the Supporting Information. The experimental self-diffusion coefficient for water is 0.23 Å^2/ps, and the infinite-dilution diffusion coefficient for the excess proton is 0.93 Å^2/ps;[57] however, the diffusion coefficients for both in a 1.7 M solution of HCl, which is the approximate concentration of our systems, are expected to be somewhat lower.[5]

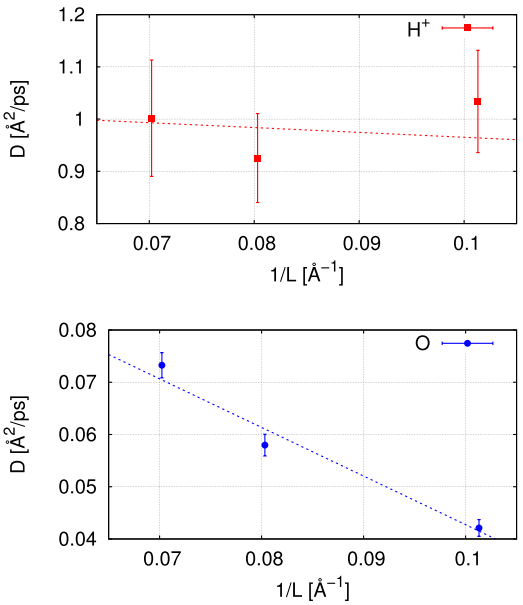

Figure 3. Diffusion coefficients for water and the excess proton as functions of the inverse box length. The error bars represent the standard errors as calculated from a boot strapping analysis of the results (see Supporting Information for details). The lines are fits to eq 1, where the fit to the excess proton data was constrained to have the same slope as that determined from the fit to the oxygen data.

It has been shown previously that hydrodynamic effects cause calculated diffusion coefficients to be suppressed when a finite simulation cell is used with periodic boundary conditions.[58,59] Specifically, the calculated diffusion coefficient for a finite size simulation is related to the value at infinite size by

$$D_{\mathrm{PBC}}(L) = D_0 - \frac{k_{\mathrm{B}}T\xi}{6\pi\eta L} \tag{1}$$

where k_{B} is Boltzmann's constant, T is the temperature of the simulaiton, ξ is a constant related to the electrostatics of the system and has a value of approximately 2.837 for cubic cells, η is the viscosity of the solvent, and L is the box length.

By fitting the data in Figure 3 to eq 1, we found D_0 = 0.14 Å^2/ps and $\eta = 6.7 \times 10^{-4}$ Pa s for water and D_0 = 1.1 Å^2/ps for the excess proton. Due to the much larger uncertainties in the calculated proton diffusion coefficients, we constrained the fit of the proton data to have the same slope as the oxygen data.

DOI: 10.1021/acs.jpcb.9b02610
J. Phys. Chem. B 2019, 123, 5536−5544

The viscosity for a 1.7 M HCl solution is approximately 1×10^{-3} Pa s.[60] The agreement here between calculated and experimental values is likely fortuitous given the over-structuring observed in the radial distribution functions; however, it does raise an important point with regard to judging the accuracy of a method for dynamic properties such as diffusion coefficients. Since all calculations are done on finite size systems, methods should be underestimating the diffusion coefficients, as the viscosity appears mostly independent of system size.[59] In the particular case of bulk water, assuming the method of interest accurately reproduces the viscosity, the calculated diffusion coefficient should be underestimated by $0.7/L$ for a box length in Å and a diffusion coefficient in Å^2/ps. For a water box with 64 molecules, this corresponds to roughly one-quarter of the limiting value.

To further analyze the dynamic properties of the systems, we calculated the mass-weighted velocity autocorrelation functions, from which the vibrational densities of states were calculated. These are shown in Figures 4 and 5. The velocity

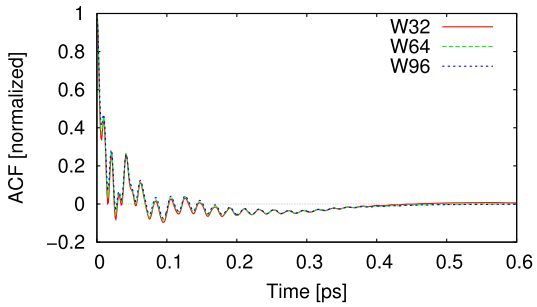

Figure 4. Mass-weighted velocity autocorrelation functions for the three systems.

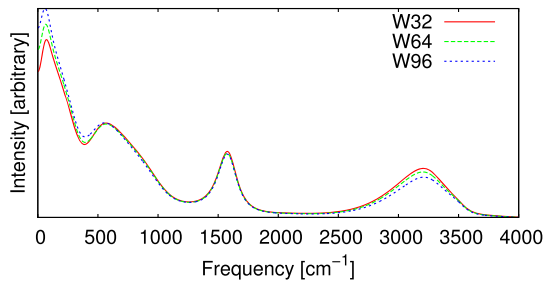

Figure 5. Vibrational densities of states calculated from the Fourier transforms of the velocity autocorrelation functions in Figure 4.

autocorrelation functions decay within about 0.5 ps, indicating that our simulations are of sufficient length to capture the vibrational dynamics of the system. Though there does not appear to be much difference between the correlation functions, the vibrational densities of states show that there are subtle changes. In particular, there is a decrease in the intensity of the stretching band and an increase in the translational band as the system size increases. These changes could be connected to the changes seen in the radial distribution functions. Overall, our results are in reasonable agreement with previous calculations of the same properties.[61]

Having established a baseline for the properties of our simulations, we now turn to the examination of correlation in the proton dynamics. In our previous work, we found that there was a higher than expected probability for the excess proton to return to its previous site as compared to a simple random walk. This finding has significant implications for the Grotthuss mechanism as the NMR and conductivity results that have served as the reference point for the time scale have been interpreted in terms of the simple random walk model.[2−4,7] As we showed previously, the use of a correlated random walk model with the experimental diffusion coefficient and the directional hopping probabilities, which we extracted from our simulations, requires that the time scale of the Grotthuss mechanism be a factor of ∼3 faster than has been quoted in the literature.[40]

This previous finding was based on molecular dynamics with only 32 molecules in our simulation cell. As was seen above, finite size effects can have an influence on calculated properties. It is reasonable to ask whether the correlations we observed in the hopping probabilities could be due, at least in part, to these finite size effects. In Figure 6, we present the

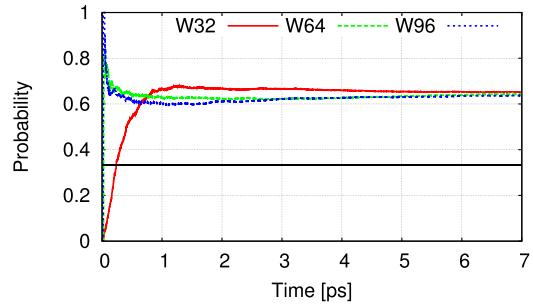

Figure 6. Cumulative moving average for the backward hopping probability. The solid black line indicates the expected probability for a simple random walk with 3 neighbors.

cumulative moving average of the calculated backward hopping probability for the three sets of simulations. The first observation is that all simulations converge to approximately the same value, indicating that there are no relevant finite size effects in contrast to the properties calculated above. In addition, we see that the calculated probability for the proton to hop backward is stable, suggesting that we are sampling from an equilibrium distribution.

To confirm that our trajectories are of sufficient length, we have calculated the same quantity using a set of 10 trajectories, each 100 ps in length. For the 100 ps trajectories, we calculated the cumulative average both for discarding just the initial picosecond of each trajectories, as we did with the 8 ps trajectories, and the first 50 ps of each trajectory. These results are shown in Figure 7, where it is clear that our sampling is sufficient, and our equilibration period appears adequate. The calculated backward hopping probability of approximately 0.63 is significantly different from the 1/3 that would be expected for a simple random walk with 3 neighbors. While our previous work demonstrated the implications of this enhanced backward hopping probability for the hopping time scale, here we explore its relationship to other findings concerning proton transfer dynamics.

Previous work by Voth and co-workers found a correlation between the presence of a fourth water molecule donating a hydrogen bond to the hydronium ion and increased long-range displacement of the positive charge.[29,30] This finding was born out of an interest in the literature in the "burst/rest" behavior of proton dynamics.[28−30,54,62] Before we move on to examining the relationship between this weak hydrogen bond donor and

DOI: 10.1021/acs.jpcb.9b02610
J. Phys. Chem. B 2019, 123, 5536−5544

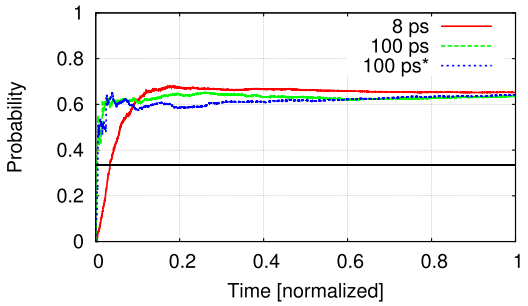

Figure 7. Comparison of the cumulative moving averages for the W32 system. The key refers to the length of the trajectories. There were 500 trajectories of 8 ps and 10 trajectories of 100 ps. For the second 100 ps result, the first 50 ps of the trajectories was discarded in order to test equilibration time. The time axis has been normalized to the lengths of the trajectories to facilitate comparison. The solid black line indicates the expected probability for a simple random walk with 3 neighbors.

the directional hopping probabilities, we would like to note that one needs to be careful not to read too much into individual trajectories or segments thereof. Diffusion of any particle or molecule is an inherently random process. Individual realizations of the random process can give a misleading view of the process as a whole.

To illustrate our point, Figure 8 displays the net displacements from a pair of trajectories. One of the trajectories is for

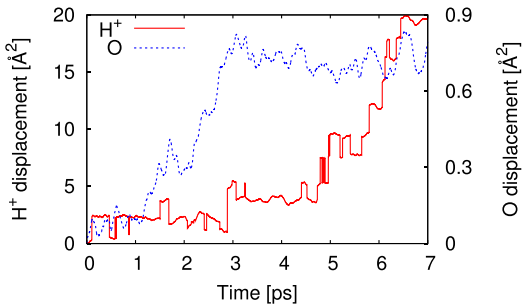

Figure 8. Net displacement of the excess proton and an oxygen atom from sample trajectories. The oxygen atom and proton data were taken from separate trajectories in the W32 set so there is no correlation between them.

the excess proton while the other is for the oxygen atom of a water molecule. In terms of the "burst/rest" paradigm, the proton trajectory could be classified as having a rest period until about 3 ps followed by a burst period. On the other hand, the oxygen trajectory could be said to have a burst period up to 3 ps followed by a rest period for the remainder of the trajectory. We note that the proton and oxygen trajectories displayed in Figure 8 come from different simulations from the W32 set so they are not correlated with each other. As the oxygen atom itself simply undergoes a normal diffusion process, it is clear that the "burst/rest" paradigm is not unique to proton dynamics but is part of the random nature of Brownian motion.

That being said, physical processes can affect the odds that a particle will experience a large displacement from its starting point, which brings us back to the correlation calculated by Voth and co-workers.[29,30] In Figure 9 we show the probability for the excess proton to hop backward conditioned on whether a fourth water molecule was donating a hydrogen bond to the

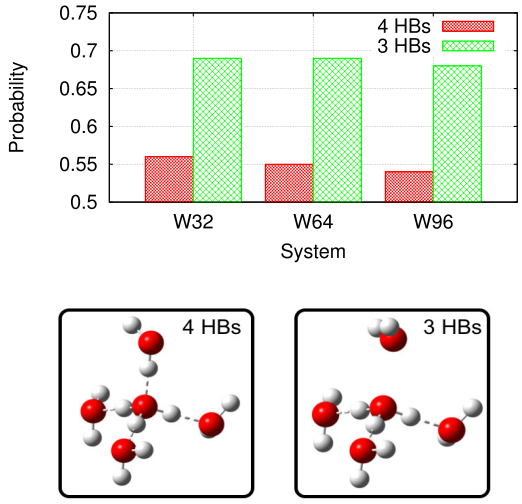

Figure 9. Probability for the excess proton to hop backward, dependent on whether there was a fourth water molecule donating a hydrogen bond to the hydronium ion at the time of the initial hop. Standard errors of the mean were all less than 0.005. The bottom panel shows schematically when a fourth water molecule is donating a hydrogen bond versus not donating.

hydronium ion before the original hop. We utilized the same criteria for the presence/absence of the fourth water molecule as Tse et al. did; namely, the closest hydrogen atom of the fourth water molecule is within 2.6 Å of the hydronium ion oxygen atom, and the angle between the vector connecting the hydronium ion oxygen atom and fourth water molecule hydrogen atom and the vector normal to the plane of the hydronium ion hydrogen atoms is less than 35°.[29]

From Figure 9 it is clear that the probability for the excess proton to return to its previous site depends on whether or not that hydronium ion was accepting a hydrogen bond when the excess proton left. This difference in the backward hopping probability provides a natural explanation for the correlation seen by Voth and co-workers[29,30] and provides support for the physical rationale given by Halle and Karlström for expecting correlation in the proton hopping directions.[4] A lower probability to return to its previous site tilts the odds in favor of the excess proton exploring new hosts and achieving a greater net displacement.

There are now established correlations between the fourth water molecule and net displacement, and between the backward hopping probability and the fourth water molecule. In order to gain further insight into the factors influencing proton dynamics, we have performed a multivariate linear regression on the net displacement with the backward hopping probability and fraction of time the fourth water molecule is donating a hydrogen bond as predictor variables. Specifically, we used

$$y_i = \beta_0 + \beta_1 x_{i1} + \beta_2 x_{i2} \quad (2)$$

to model our data, where y_i is the net displacement of the proton at the end of the ith proton trajectory, x_{i1} is the average backward hopping probability for the ith proton trajectory, x_{i2} is the fraction of time the fourth water molecule was donating a hydrogen bond to the hydronium ion in the ith trajectory, and β_j are our regression coefficients.

As can be seen in Table 1, the backward hopping probability has a larger regression coefficient, indicating that changes to

DOI: 10.1021/acs.jpcb.9b02610
J. Phys. Chem. B 2019, 123, 5536−5544

Table 1. Regression Coefficients and Their *p*-Values from Multivariate Linear Regressions on the Net Displacements with the Backward Hopping Probabilities and Fraction of Time the Fourth Water Molecule Is Donating a Hydrogen Bond as Predictor Variables

variable	regression coeff	std error	*p*-value
	W32		
hop probability	−12.083	1.708	5.13×10^{-12}
fourth water	3.509	1.856	5.92×10^{-2}
	W64		
hop probability	−13.364	1.715	3.88×10^{-14}
fourth water	5.098	1.867	6.551×10^{-3}
	W96		
hop probability	−10.797	1.706	5.51×10^{-10}
fourth water	1.001	1.852	5.89×10^{-1}

this parameter have a stronger influence on the net displacement, and a lower *p*-value, indicating higher confidence that this parameter is important. Scatter plots of the analyzed data can be found in the Supporting Information. These results show that a large part of the correlation seen by Voth and coworkers is due to the correlation we found between the hopping probability and the fourth water molecule, with the hopping probability influencing the net displacement. The relative importance of the backward hopping probability over the presence of the fourth water molecule for directly influencing the net displacement of the proton can be seen in the change in regression coefficients for the variables on going from univariate regressions to the multivariate regression presented above. The details are given in the Supporting Information, but the main result is that the regression coefficient for the hopping probability changes by only 8.8% on average while the same for the fourth water molecule decreases by 96% on average.

We note that the correlation between the backward hopping probability and the number of hydrogen bonds to the hydronium ion is robust to simulation parameters, as can be seen in Table 2. Here we have computed the same quantities for 32 molecule simulations run with different exchange-correlation functionals and at higher wave function and charge density cutoffs. The simulations with alternative functionals only included 10 independent trajectories, resulting in the larger standard errors of the means. The rest of the parameters for these simulations were the same as those discussed previously. While there is some variability in the values for the probabilities, the trend of a lower backward hopping probability when there was a fourth water molecule present holds across all of the functionals. The smaller number of independent trajectories in these sets does not allow for a meaningful regression analysis like we did for the main data; however, we have no reason to believe the results would be substantially different for the other functionals.

Table 2. Functional Dependence of the Probability for the Excess Proton to Hop Backwards Dependent on Whether There was a Fourth Water Molecule Donating a Hydrogen Bond to the Hydronium Ion at the Time of the Initial Hop[a]

	4 HBs	3 HBs
PBE	0.67 [0.02]	0.73 [0.01]
PBE-D2	0.50 [0.02]	0.68 [0.01]
revPBE	0.50 [0.03]	0.71 [0.01]
BLYP	0.53 [0.03]	0.67 [0.01]
BLYP-D2	0.62 [0.02]	0.71 [0.01]
optB88	0.59 [0.02]	0.69 [0.01]

[a]The numbers in brackets give the standard errors of the means.

In our previous work, we pointed out that correlation in the proton hopping directions would have a direct and substantial impact on the time scale of the Grotthuss mechanism that is extracted from the measured diffusion coefficient via a random walk model.[40] We showed that the correlations we observed in our simulations would translate into a time scale of approximately 0.5 ps in contrast to the ∼1.5 ps commonly reported.[1,7] However, a recent series of vibrational spectroscopy studies have measured relaxation times between 0.48 and 2.5 ps, concluding that proton transfer occurs in 1−2 ps.[35,37,38] The interpretation of these results did not rely on a random walk model and, therefore, appears to contradict our results.

We postulate that this apparent discrepancy can be resolved by carefully examining which types of proton hops are being considered. Carpenter et al. remarked that the decay dynamics they observed arose from proton-transfer-related reorganization of the hydrogen bond connectivity of the liquid water.[37] Halle and Karlström put forth that correlation in the proton hopping direction would be a consequence of the hydrogen bond connectivity of the surrounding water molecules not adjusting to a change in the proton host site before another hop occurs.[4] This suggests, as would be inferred from Carpenter et al. stating that their measured time scale corresponds to irreversible proton hopping, that the spectroscopy may be insensitive to proton hops that are not accompanied by an overall rearrangement of the hydrogen bonding network. As we have accounted for all proton hops in our simulation, it is then not surprising that we obtained a different time scale.

To quantify irreversible proton hopping in our simulations, we have calculated the ratio of the total number of proton hops and the number of irreversible proton hops over 5 ps segments of our trajectories. Here we define an "irreversible" proton hop as one after which the same hydronium ion does not re-form for at least 2 ps. These results are presented in Tables 3 and 4.

Table 3. Ratio of the Total Number of Proton Hops per Proton per Trajectory and the Number of Irreversible Proton Hops per Proton per Trajectory[a]

	total/irrevisible
W32	5.7 [0.1]
W64	5.0 [0.1]
W96	4.7 [0.1]

[a]The numbers in brackets give the standard errors of the means. An irreversible hop is defined as one after which the proton does not return to that site for at least 2 ps.

As can be seen in the tables, there are roughly a factor of 5 fewer irreversible hops. Using our set of 100 ps trajectories, we checked the convergence of this ratio. With the same 2 ps window during which the same hydronium ion cannot re-form to be considered an irreversible hop, we obtained a ratio of 5.7 [0.2], exactly in agreement with the set of shorter trajectories. If we assume that the time scale for irreversible hopping is scaled by a similar factor relative to the time scale for all hopping, then we arrive at a time scale of approximately 2.5 ps

DOI: 10.1021/acs.jpcb.9b02610
J. Phys. Chem. B 2019, 123, 5536−5544

Table 4. Functional Dependence of the Ratio of the Total Number of Proton Hops per Proton per Trajectory and the Number of Irreversible Proton Hops per Proton per Trajectory[a]

	total/irrevisible
PBE	8.0 [2.0]
PBE-D2	4.5 [0.8]
revPBE	4.6 [0.7]
BLYP	5.1 [1.1]
BLYP-D2	5.2 [0.8]
optB88	4.4 [0.8]

[a]The numbers in brackets give the standard errors of the means. An irreversible hop is defined as one after which the proton does not return to that site for at least 2 ps.

for irreversible hopping given that we estimated a time scale of ~0.5 ps when accounting for all hopping.[40]

This 2.5 ps time scale is in reasonable agreement with the vibrational spectroscopy results, and it is further supported if we look back to the model of the NMR relaxation rate derived by Halle and Karlström.[4] Their model gives the proton hopping time scale τ as

$$\tau = \frac{1 - q}{(1 + \gamma)c_w k_+} \quad (3)$$

where q is the probability to hop backward, γ is the number of re-encounters of the proton with a given oxygen atom, c_w is the concentration of water, and k_+ is the NMR measured relaxation rate. For irreversible hopping, $q = 0$ and $\gamma = 0$; at infinite dilution $c_w = 55.3$ M, and Halle and Karlström measured $k_+ = 7.1 \times 10^{-3}$ M^{-1} ps^{-1}.[3,4] Combined, these give a time scale of 2.5 ps, in agreement with the other results.

Finally, we noted in our previous work that we could not rule out the elevated hopping probability being due to concentration effects.[40] While the additional simulations we performed for the current work were all at the same concentration, the W64 and W96 simulations included multiple excess protons in the same simulation cell, allowing us to interrogate for interactions between them. Shown in Figure 10 is a histogram of the probability for a proton to hop backward as a function of the distance between hydronium ions. As can be seen, there is essentially no distance dependence for the hopping probability. This indicates that there are no relevant direct interactions between excess protons; any concentration effects would have to be indirect through the disruption of the solvent hydrogen bonding network. Since our previous work showed that the backward hopping probability decreased upon increasing the temperature of the simulation, we can conclude that the backward hopping probability would not be likely to decrease when moving to more dilute solutions where there would be more structure to the hydrogen bond network. However, additional simulations at different concentrations are needed to confirm any results concerning concentration dependence.

CONCLUSIONS

Expanding upon our previous simulations, we have shown that the elevated backward hopping probability for the excess proton is not an artifact of simulation size. Furthermore, we demonstrated that the presence of a fourth water molecule, donating a hydrogen bond to the hydronium ion at the time the excess proton leaves, results in a decreased probability for

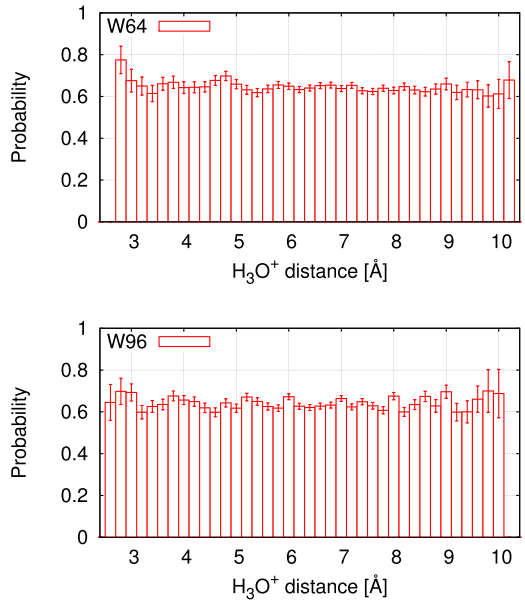

Figure 10. Probability for the excess proton to return to its previous site as a function of the distance between that previous hydronium ion and its nearest hydronium ion at the time of the original hop. Note that, for W32 with only one excess proton per simulation cell, the hydronium ion is always the same distance (~9.87 Å) from its image so results for W32 are not shown.

the proton to return to that host water molecule. This finding offers a natural explanation of the correlation between the hydronium ion accepting a hydrogen bond and the net displacement of the proton observed by Voth and co-workers.[29,30] Furthermore, we showed through a multivariate linear regression that the backward hopping probability has the stronger influence on the net displacement of the proton, and the correlation between the fourth water molecule and net displacement is mediated through the hopping probability.

We then showed how our simulations are compatible with the spectroscopic measurements of Tokmakoff and co-workers.[35,37,38] This is based on recognizing that not all proton hops are accompanied by a complete reorganization of the hydrogen bond network. When we consider only irreversible protons hops in our simulations, we obtain a time scale consistent with the longer one proposed in the vibrational spectroscopy experiments and consistent with the NMR measurement of the time scale when interpreted in terms of irreversible protons hops. This highlights the need for precision when discussing proton transitions, much like Tse et al. highlighted the need for precision in discussing concerted hopping.[29]

Finally, we offered evidence that the observed elevated backward hopping probability may not be due to the relatively high concentration of our simulation setup. The probability to hop backward is insensitive to the distance between the excess protons. Additionally, our previous results at different temperatures showed that the backward hopping probability decreased with increasing temperature, indicating that disruptions to the hydrogen bonding network caused by additional acid molecules would potentially move proton hopping toward the simple random walk limit. Of course, once the concentration increases sufficiently such that there are not enough water molecules to solvate all of the hydronium ions, the dynamics could be substantially different.

DOI: 10.1021/acs.jpcb.9b02610
J. Phys. Chem. B 2019, 123, 5536−5544

■ ASSOCIATED CONTENT

Supporting Information

The Supporting Information is available free of charge on the ACS Publications website at DOI: 10.1021/acs.jpcb.9b02610.

Radial distribution functions, mean squared displacements, diffusion coefficients, and details of the regression analyses for the studied systems (PDF)

■ AUTHOR INFORMATION

Corresponding Author

*E-mail: sean.fischer@nrl.navy.mil. Phone: 202-404-1687.

ORCID

Sean A. Fischer: 0000-0003-2242-6654

Notes

The authors declare no competing financial interest.

■ ACKNOWLEDGMENTS

The authors acknowledge support from the U.S. Office of Naval Research through the U.S. Naval Research Laboratory.

■ REFERENCES

(1) Agmon, N.; Bakker, H. J.; Campen, R. K.; Henchman, R. H.; Pohl, P.; Roke, S.; Thämer, M.; Hassanali, A. Protons and Hydroxide Ions in Aqueous Systems. *Chem. Rev.* **2016**, *116*, 7642−7672.

(2) Meiboom, S. Nuclear Magnetic Resonance Study of the Proton Transfer in Water. *J. Chem. Phys.* **1961**, *34*, 375−388.

(3) Halle, B.; Karlström, G. Prototropic Charge Migration in Water Part 1. Rate Constants in Light and Heavy Water and in Salt Solutions from Oxygen-17 Spin Relaxation. *J. Chem. Soc., Faraday Trans. 2* **1983**, *79*, 1031−1046.

(4) Halle, B.; Karlström, G. Prototropic Charge Migration in Water Part 2. Interpretation of Nuclear Magnetic Resonance and Conductivity Data in Terms of Model Mechanisms. *J. Chem. Soc., Faraday Trans. 2* **1983**, *79*, 1047−1073.

(5) Dippel, T.; Kreuer, K. D. Proton Transport Mechanism in Concentrated Aquesous Solutions and Solid Hydrates of Acids. *Solid State Ionics* **1991**, *46*, 3−9.

(6) Kreuer, K. D. Proton Conductivity: Materials and Applications. *Chem. Mater.* **1996**, *8*, 610−641.

(7) Agmon, N. The Grotthuss Mechanism. *Chem. Phys. Lett.* **1995**, *244*, 456−462.

(8) Tuckerman, M.; Laasonen, K.; Sprik, M.; Parrinello, M. Ab Initio Molecular Dynamics Simulation of the Solvation and Transport of Hydronium and Hydroxyl Ions in Water. *J. Chem. Phys.* **1995**, *103*, 150−161.

(9) Tuckerman, M.; Laasonen, K.; Sprik, M.; Parrinello, M. Ab Initio Molecular Dynamics Simulation of the Solvation and Transport of H_3O^+ and OH^- Ions in Water. *J. Phys. Chem.* **1995**, *99*, 5749−5752.

(10) Marx, D.; Tuckerman, M. E.; Hutter, J.; Parrinello, M. The Nature of the Hydrated Excess Proton in Water. *Nature* **1999**, *397*, 601−604.

(11) Schmitt, U. W.; Voth, G. A. The Computer Simulation of Proton Transport in Water. *J. Chem. Phys.* **1999**, *111*, 9361−9381.

(12) Day, T. J. F.; Schmitt, U. W.; Voth, G. A. The Mechanism of Hydrated Proton Transport in Water. *J. Am. Chem. Soc.* **2000**, *122*, 12027−12028.

(13) Lapid, H.; Agmon, N.; Petersen, M. K.; Voth, G. A. A Bond-Order Analysis of the Mechanism for Hydrated Proton Mobility in Liquid Water. *J. Chem. Phys.* **2005**, *122*, 014506.

(14) Cukierman, S. Et tu, Grotthuss! and Other Unfinished Stories. *Biochim. Biophys. Acta, Bioenerg.* **2006**, *1757*, 876−885.

(15) Botti, A.; Bruni, F.; Ricci, M. A.; Soper, A. K. Eigen Versus Zundel Complexes in HCl-Water Mixtures. *J. Chem. Phys.* **2006**, *125*, 014508.

(16) Winter, B.; Faubel, M.; Hertel, I. V.; Pettenkofer, C.; Bradforth, S. E.; Jagoda-Cwiklik, B.; Cwiklik, L.; Jungwirth, P. Electron Binding Energies of Hydrated H_3O^+ and OH^-: Photoelectron Spectroscopy of Aqueous Acid and Base Solutions Combined with Electronic Structure Calculations. *J. Am. Chem. Soc.* **2006**, *128*, 3864−3865.

(17) Woutersen, S.; Bakker, H. J. Ultrafast Vibrational and Structural Dynamics of the Proton in Liquid Water. *Phys. Rev. Lett.* **2006**, *96*, 138305.

(18) Amir, W.; Gallot, G.; Hache, F.; Bratos, S.; Leicknam, J.-C.; Vuilleumier, R. Time-Resolved Observation of the Eigen cation in Liquid Water. *J. Chem. Phys.* **2007**, *126*, 034511.

(19) Marx, D. Proton Transfer 200 Years after von Grotthuss: Insights from Ab Initio Simulations. *ChemPhysChem* **2006**, *7*, 1848−1870.

(20) Chandra, A.; Tuckerman, M. E.; Marx, D. Connecting Solvation Shell Structure to Proton Transport Kinetics in Hydrogen-Bonded Networks via Population Correlation Functions. *Phys. Rev. Lett.* **2007**, *99*, 145901.

(21) Tuckerman, M. E.; Chandra, A.; Marx, D. A Statistical Mechanical Theory of Proton Transport Kinetics in Hydrogen-Bonded Networks Based on Population Correlation Functions with Applications to Acids and Bases. *J. Chem. Phys.* **2010**, *133*, 124108.

(22) Markovitch, O.; Chen, H.; Izvekov, S.; Paesani, F.; Voth, G. A.; Agmon, N. Special Pair Dance and Partner Selection: Elementary Steps in Proton Transport in Liquid Water. *J. Phys. Chem. B* **2008**, *112*, 9456−9466.

(23) Tielrooij, K. J.; Timmer, R. L. A.; Bakker, H. J.; Bonn, M. Structure Dynamics of the Proton in Liquid Water Probed with Terahertz Time-Domain Spectroscopy. *Phys. Rev. Lett.* **2009**, *102*, 198303.

(24) Berkelbach, T. C.; Lee, H.-S.; Tuckerman, M. E. Concerted Hydrogen-Bond Dynamics in the Transport Mechanism of the Hydrated Proton: A First Principles Molecular Dynamics Study. *Phys. Rev. Lett.* **2009**, *103*, 238302.

(25) Stoyanov, E. S.; Stoyanova, I. V.; Reed, C. A. The Structure of the Hydrogen Ion (H^+_{aq}) in Water. *J. Am. Chem. Soc.* **2010**, *132*, 1484−1485.

(26) Xu, J.; Zhang, Y.; Voth, G. A. Infrared Spectrum of the Hydrated Proton in Water. *J. Phys. Chem. Lett.* **2011**, *2*, 81−86.

(27) Knight, C.; Voth, G. A. The Curious Case of the Hydrated Proton. *Acc. Chem. Res.* **2012**, *45*, 101−109.

(28) Hassanali, A.; Giberti, F.; Cuny, J.; Kühne, T. D.; Parrinello, M. Proton Transfer Through the Water Gossamer. *Proc. Natl. Acad. Sci. U. S. A.* **2013**, *110*, 13723−13728.

(29) Tse, Y.-L. S.; Knight, C.; Voth, G. A. An Analysis of Hydrated Proton Diffusion in Ab Initio Molecular Dynamics. *J. Chem. Phys.* **2015**, *142*, 014104.

(30) Biswas, R.; Tse, Y.-L. S.; Tokmakoff, A.; Voth, G. A. Role of Presolvation and Anharmonicity in Aqueous Phase Hydrated Proton Solvation and Transport. *J. Phys. Chem. B* **2016**, *120*, 1793−1804.

(31) Chen, C.; Arntsen, C.; Voth, G. A. Development of Reactive Force Fields using Ab Initio Molecular Dynamics Simulation Minimally Biased to Experimental Data. *J. Chem. Phys.* **2017**, *147*, 161719.

(32) Decka, D.; Schwaab, G.; Havenith, M. A THz/FTIR Fingerprint of the Solvated Proton: Evidence for Eigen Structure and Zundel Dynamics. *Phys. Chem. Chem. Phys.* **2015**, *17*, 11898−11907.

(33) Dahms, F.; Fingerhut, B. P.; Nibbering, E. T. J.; Pines, E.; Elsaesser, T. Large-Amplitude Transfer Motion of Hydrated Excess Protons Mapped by Ultrafast 2D IR Spectroscopy. *Science* **2017**, *357*, 491−495.

(34) Daly, C. A., Jr.; Streacker, L. M.; Sun, Y.; Pattenaude, S. R.; Hassanali, A. A.; Petersen, P. B.; Corcelli, S. A.; Ben-Amotz, D. Decomposition of the Experimental Raman and Infrared Spectra of Acidic Water in Proton, Special Pair, and Counterion Contributions. *J. Phys. Chem. Lett.* **2017**, *8*, 5246−5252.

(35) Thämer, M.; De Marco, L.; Ramasesha, K.; Mandal, A.; Tokmakoff, A. Ultrafast 2D IR Spectroscopy of the Excess Proton in Liquid Water. *Science* **2015**, *350*, 78−82.
(36) Biswas, R.; Carpenter, W.; Fournier, J. A.; Voth, G. A.; Tokmakoff, A. IR Spectral Assignments for the Hydrated Excess Proton in Liquid Water. *J. Chem. Phys.* **2017**, *146*, 154507.
(37) Carpenter, W. B.; Fournier, J. A.; Lewis, N. H. C.; Tokmakoff, A. Picosecond Proton Transfer Kinetics in Water Revealed with Ultrafast IR Spectroscopy. *J. Phys. Chem. B* **2018**, *122*, 2792−2802.
(38) Fournier, J. A.; Carpenter, W. B.; Lewis, N. H. C.; Tokmakoff, A. Broadband 2D IR Spectroscopy Reveals Dominant Asymmetric $H_5O_2^+$ Proton Hydration Structures in Acid Solutions. *Nat. Chem.* **2018**, *10*, 932−937.
(39) Chen, M.; Zheng, L.; Santra, B.; Ko, H.-Y.; DiStasio, R. A., Jr.; Klein, M. L.; Car, R.; Wu, X. Hydroxide Diffuses Slower than Hydronium in Water because its Solvated Structure Inhibits Correlated Proton Transfer. *Nat. Chem.* **2018**, *10*, 413−419.
(40) Fischer, S. A.; Dunlap, B. I.; Gunlycke, D. Correlated Dynamics in Aqueous Proton Diffusion. *Chem. Sci.* **2018**, *9*, 7126−7132.
(41) Giannozzi, P.; Baroni, S.; Bonini, N.; Calandra, M.; Car, R.; Cavazzoni, C.; Ceresoli, D.; Chiarotti, G. L.; Cococcioni, M.; Dabo, I.; et al. QUANTUM ESPRESSO: A Modular and Open-Source Software Project for Quantum Simulations of Materials. *J. Phys.: Condens. Matter* **2009**, *21*, 395502.
(42) Perdew, J. P.; Burke, K.; Ernzerhof, M. Generalized Gradient Approximation Made Simple. *Phys. Rev. Lett.* **1996**, *77*, 3865−3868.
(43) Vanderbilt, D. Soft Self-Consistent Pseudopotentials in a Generalized Eigenvalue Formalism. *Phys. Rev. B: Condens. Matter Mater. Phys.* **1990**, *41*, 7892−7895.
(44) Laasonen, K.; Car, R.; Lee, C.; Vanderbilt, D. Implementation of Ultrasoft Pseudopotentials in Ab Initio Molecular Dynamics. *Phys. Rev. B: Condens. Matter Mater. Phys.* **1991**, *43*, 6796−6799.
(45) Laasonen, K.; Pasquarello, A.; Car, R.; Lee, C.; Vanderbilt, D. Car-Parrinello Molecular Dynamics with Vanderbilt Ultrasoft Pseudopotentials. *Phys. Rev. B: Condens. Matter Mater. Phys.* **1993**, *47*, 10142−10153.
(46) Yoo, S.; Zeng, X. C.; Xantheas, S. S. On the Phase Diagram of Water with Density Functional Theory Potentials: The Melting Temperature of Ice I_h with the Perdew-Burke-Ernzerhof and Becke-Lee-Yang-Parr Functionals. *J. Chem. Phys.* **2009**, *130*, 221102.
(47) Gillan, M. J.; Alfè, D.; Michaelides, A. Perspective: How Good is DFT for Water. *J. Chem. Phys.* **2016**, *144*, 130901.
(48) Car, R.; Parrinello, M. Unified Approach for Molecular Dynamics and Density-Functional Theory. *Phys. Rev. Lett.* **1985**, *55*, 2471−2474.
(49) Grimme, S. Semiempirical GGA-Type Density Functional Constructed with a Long-Range Dispersion Correction. *J. Comput. Chem.* **2006**, *27*, 1787−1799.
(50) Barone, V.; Casarin, M.; Forrer, D.; Pavone, M.; Sambi, M.; Vittadini, A. Role and Effective Treatment of Dispersive Forces in Materials: Polyethylene and Graphite Crystals as Test Cases. *J. Comput. Chem.* **2009**, *30*, 934−939.
(51) Zhang, Y.; Yang, W. Comment on "Generalized Gradient Approximation Made Simple. *Phys. Rev. Lett.* **1998**, *80*, 890.
(52) Becke, A. D. Density-Functional Exchange-Energy Approximation with Correct Asymptotic Behavior. *Phys. Rev. A* **1988**, *38*, 3098−3100.
(53) Lee, C.; Yang, W.; Parr, R. G. Development of the Colle-Salvetti Correlation-Energy Formula into a Functional of the Electron Density. *Phys. Rev. B: Condens. Matter Mater. Phys.* **1988**, *37*, 785−789.
(54) Wu, Y.; Chen, H.; Wang, F.; Paesani, F.; Voth, G. A. An Improved Multistate Empirical Valence Bond Model for Aqueous Proton Solvation and Transport. *J. Phys. Chem. B* **2008**, *112*, 467−482.
(55) Kühne, T. D.; Krack, M.; Parrinello, M. Static and Dynamic Properties of Liquid Water from First Principles by a Novel Car-Parrinello-like Approach. *J. Chem. Theory Comput.* **2009**, *5*, 235−241.
(56) Soper, A. K. The Radial Distribution Functions of Water as Derived from Radiation Total Scattering Experiments: Is There Anything We Can Say for Sure? *ISRN Phys. Chem.* **2013**, *2013*, 279463.
(57) Mills, R.; Lobo, V. M. M. *Self-Diffusion in Electrolyte Solutions: A Critical Examination of Data Compiled from the Literature*; Physical Sciences Data; Elsevier: New York, NY, 1989; Vol. *36*.
(58) Dünweg, B.; Kremer, K. Molecular Dynamics Simulation of a Polymer Chain in Solution. *J. Chem. Phys.* **1993**, *99*, 6983−6997.
(59) Yeh, I.-C.; Hummer, G. System-Size Dependence of Diffusion Coefficients and Viscosities from Molecular Dynamics Simulations with Periodic Boundary Conditions. *J. Phys. Chem. B* **2004**, *108*, 15873−15879.
(60) Nishikata, E.; Ishii, T.; Ohta, T. Viscosities of Aqueous Hydrochloric Acid Solutions, and Densities and Viscosities of Aqueous Hydroiodic Acid Solutions. *J. Chem. Eng. Data* **1981**, *26*, 254−256.
(61) Corongiu, G.; Clementi, E. Molecular Dynamics Simulations with a Flexible and Polarizable Potential: Density of States for Liquid Water at Different Temperatures. *J. Chem. Phys.* **1993**, *98*, 4984−4990.
(62) Hassanali, A. A.; Giberti, F.; Sosso, G. C.; Parrinello, M. The Role of the Umbrella Inversion Mode in Proton Diffusion. *Chem. Phys. Lett.* **2014**, *599*, 133−138.

DOI: 10.1021/acs.jpcb.9b02610
J. Phys. Chem. B 2019, 123, 5536−5544